ЖЭТФ, 2011, том 139, вып. 1, стр. 75–89

PHOTON EMISSION FROM BARE QUARK STARS

B. G. Zakharov *

Landau Institute for Theoretical Physics, Russian Academy of Sciences
117334, Moscow, Russia

Received May 11, 2010

We investigate the photon emission from the electrosphere of a quark star. We show that at temperatures $T \approx 0.1$–1 MeV, the dominating mechanism is the bremsstrahlung due to bending of electron trajectories in the mean Coulomb field of the electrosphere. The radiated energy for this mechanism is much larger than that for the Bethe–Heitler bremsstrahlung. The energy flux from the mean field bremsstrahlung also exceeds the one from the tunnel e^+e^- pair creation. We demonstrate that the LPM suppression of the photon emission is negligible.

1. INTRODUCTION

The hypothesis of quark stars made of stable strange quark matter (SQM) [1–3] has been attracting much attention for many years. It is possible that quark stars (if they exist) may be (at least in the initial hot stage) without a crust of normal matter [4]. In contrast to neutron stars, the density of SQM for bare quark stars should drop abruptly at the scale ~ 1 fm. The SQM in the normal phase and in the two-flavor superconducting (2SC) phase should also contain electrons (for the normal phase, the electron chemical potential μ is about 20 MeV [2, 5]). In contrast to the quark density, the electron density decreases smoothly above the star surface at the scale $\sim 10^3$ fm [2, 5]. For the star surface temperature $T \ll \mu$, e. g. $T \lesssim 10^{10}$ K ~ 1 MeV, this "electron atmosphere" (usually called the electrosphere) may be regarded as a strongly degenerate relativistic electron gas [2, 5].

From the standpoint of distinguishing bare quark stars from neutron stars, it is very important to have theoretical predictions for the photon emission from bare quark stars. Unlike for neutron stars (or quark stars with a crust of normal matter), the photon emission from quark stars made of stable self-bound SQM may potentially exceed the Eddington limit. This fact may be used for detecting a bare quark star. However, the SQM itself is a very poor emitter at $T \ll \omega_p^q$ [6, 7] (here, $\omega_p^q \approx 20$ MeV is the plasma frequency of SQM [6]). At such temperatures, the photon emission from the quark surface is a tunnel process, and the radiation rate turns out to be negligibly small compared to the black body radiation [6]. However, for the electrosphere, the plasma frequency ω_p^e is much smaller than that for the SQM. Therefore, the photon emission from the electrosphere may potentially dominate the luminosity of a quark star. For understanding the prospects of detecting bare quark stars, it is highly desirable to have quantitative predictions for the photon emission from the electrosphere. This is also interesting in the context of the scenario of gamma-ray repeaters due to reheating of a quark star by the impact of a massive comet-like object [8], and the dark matter model in the form of matter/antimatter SQM nuggets [9].

An obvious candidate for the photon emission from the electrosphere is the bremsstrahlung from electrons. It may be due to either the electron–electron interaction (the Bethe–Heitler bremsstrahlung) or the interaction of electrons with the mean electric field of the electrosphere. One more mechanism is related to the tunnel e^+e^- pair creation [4, 10]. The point is that the electric field of the electrosphere must be very strong. It may be about several tens of the critical field for the tunnel Schwinger pair production $E_{cr} = m_e^2/e$ [11] (we use the units where $c = \hbar = k_B = 1$). In this scenario, the photons appear through e^+e^- annihilation in the outflowing $e^\pm$ wind [12].

The bremsstrahlung from the electrosphere due to the electron–electron interaction has been addressed in [13, 14]. The authors of [13] used the soft-photon approximation and factored the $e^-e^- \to e^-e^-$ cross section in the spirit of Low's theorem. In [14], it was

*E-mail: bgz@itp.ac.ru

pointed out that this approximation is inadequate because it neglects the effect of the photon energy on the electron Pauli blocking, which should lead to a strong suppression of the radiation rate. But the authors of [14] did not treat this problem consistently either. To take the effect of the minimal photon energy into account, they suggested some restrictions on the initial electron momenta imposed by hand. Thus they obtained the radiated energy flux from the $e^-e^- \to e^-e^-\gamma$ process that was much smaller than that in [13] and than the energy flux from the tunnel e^+e^- pair creation [4, 10]. In [15], the first attempt was made to include the effect of the mean Coulomb field of the electrosphere on the photon emission. The authors obtained a considerable enhancement of the radiation rate. But similarly to [13], the analysis in [15] treated the Pauli blocking effect incorrectly. We also note that the photon quasiparticle mass was neglected in [14, 15]. As we show in what follows, this approximation is clearly inadequate because the finite photon mass suppresses the radiation rate strongly.

Therefore, the theoretical situation with the photon bremsstrahlung from the electrosphere is still controversial and uncertain. The main problem here, which was not solved in the previous analyses [13–15], is an accurate account for the photon energy in the electron Pauli blocking. In this paper, we address the bremsstrahlung from the electrosphere in a way similar to the Arnold–Moore–Yaffe (AMY) [16] approach to the collinear photon emission from a hot quark–gluon plasma based on the thermal field theory. We use a reformulation of the AMY formalism given in [17]. It is based on the light-cone path integral (LCPI) approach [18–20] (see [21, 22] for reviews) to in-medium radiation processes. For an infinite homogeneous plasma (with zero mean field), the formalism in [17] reproduces the AMY results [16]. The LCPI formulation in [17] has the advantage that it also works for plasmas with a nonzero mean field. It allows evaluating the photon emission accounting for bending of the electron trajectories in the mean Coulomb potential of the electrosphere. Contrarily to very crude and qualitative methods in [13–15], the treatment of the Pauli blocking effects in [16, 17] has robust quantum field theoretical grounds. Of course, our approach is only valid in the regime of collinear photon emission when the dominating photon energies exceed several units of the photon quasiparticle mass. Numerical calculations show that even at $T \sim 0.1$ MeV, the effect of noncollinear configurations is relatively small.

We demonstrate that for the temperatures $T \approx 0.1$–1 MeV, the radiated energy flux from the $e^- \to e^-\gamma$ transition in the mean electric field is much larger than that from the Bethe–Heitler bremsstrahlung. It also exceeds the energy flux from the tunnel e^+e^- pairs. We also demonstrate that contrary to conclusions in [13], the Landau–Pomeranchuk–Migdal (LPM) suppression [23, 24] of photon bremsstrahlung is negligible. Our results show that the photon emission from the electrosphere may be of the same order as the black body radiation. Therefore, the situation with distinguishing a bare quark star made of SQM in the normal (or 2SC) phase from a neutron star using the luminosity [4, 25] may be more optimistic than in the scenario with the tunnel e^+e^- pair creation [4].

The results of this work were briefly described in [26]. In this paper, we present our results in a more detailed form. The plan of the paper is as follows. In Sec. 2, we review the basic formulas and approximations. In Sec. 3, we discuss the evaluation of photon emission from a given electron in the electromagnetic field of the electrosphere, which includes both the mean Coulomb field and the ordinary fluctuation field generated by neighboring electrons. In Sec. 4, we present numerical results for the radiated energy flux. Section 5 is devoted to the conclusions.

2. BASIC FORMULAS AND APPROXIMATIONS

For the electrosphere, as in Refs. [4, 13, 14], we use the model of a relativistic strongly degenerate electron gas in the Thomas–Fermi approximation. In this approximation, the local electron number density is given by

$$n_e(h) = \frac{\mu^3(h)}{3\pi^2},$$

where h is the distance from the quark surface. The h dependence of the chemical potential is governed by the Poisson equation for the electrostatic potential $V = \mu/e$. For $h > 0$, this gives [2, 5]

$$\mu(h) = \frac{\mu(0)}{(1 + h/H)}\,, \tag{1}$$

where

$$H = \sqrt{3\pi/2\alpha}/\mu(0), \quad \alpha = e^2/4\pi.$$

We assume that the electrosphere is optically thin. This means that the photon absorption and stimulated emission can be neglected. In this regime, the luminosity may be expressed in terms of the energy radiated spontaneously per unit time and volume, usually called the emissitivity Q. In the formalism in [17], the emissitivity per unit photon energy ω at a given h can be written as

$$\frac{dQ(h,\omega)}{d\omega} = \frac{\omega(k)}{4\pi^3}\frac{dk}{d\omega} \times$$
$$\times \int \frac{d\mathbf{p}}{p} n_F(E)[1-n_F(E')]\theta(p-k)\frac{dP(\mathbf{p},x)}{dx\,dL}, \quad (2)$$

where k denotes the photon momentum, E and E' are the electron energies before and after the photon emission,

$$n_F(E) = [\exp((E-\mu)/T)+1]^{-1}$$

is the local electron Fermi distribution (we omit the argument h in the functions in the right-hand side of (2)), and $x = k/p$ is the photon longitudinal (along the initial electron momentum $\mathbf{p}$) fractional momentum. The function $dP/dx\,dL$ in (2) is the probability of the photon emission per unit x and length from an electron in the potential generated by other electrons, which includes both the smooth collective Coulomb field and the usual fluctuating plasma part related to the field generated by the neighboring electrons. We note that formula (2) accounts for photons emitted to all directions, because in an optically thin electrosphere, practically all the photons radiated to the hemisphere directed to the quark surface are reflected either in the electrosphere (at the level with $\omega_p^e = \omega$) or from the quark surface. Only the photons with $\omega \gtrsim \omega_p^q \approx 20$ MeV may be absorbed in the quark matter. But such photons are not important at temperatures $T \lesssim 1$ MeV considered in this paper. For the above reasons, it would be incorrect to exclude the photons emitted toward the star surface, as was done in [14].

Our basic formula (2) assumes that the photon emission is a local process, i. e., the photon formation length (denoted by l_f) is small compared to the thickness of the electrosphere[1)]. Evidently, only in this case a local emissitivity can be defined. We note that Eq. (2) defines the rate of photon production at a given photon energy, which remains constant during the photon propagation in the electrosphere. The photon momentum in this process changes adiabatically according to the photon quasiparticle dispersion relation in the electron plasma. Also, formula (2) assumes that on the scale $\sim l_f$, the electron trajectories are smooth. This means that besides the evident condition $l_f \ll R_m$ (where R_m is the curvature radius of the electron trajectory in the mean field), the typical scattering angle related to the random walk of an electron due to electron–electron interaction should also be small. It can be shown that these conditions are satisfied for the electrosphere. An important consequence of the smoothness of electron trajectories at the scale $\sim l_f$ is the longitudinal factorization of the Pauli blocking factor $1-n_F(E')$ for the final state of the radiating electron in (2). Just the fact that the trajectories are smooth in the process of photon emission allows neglecting the statistics effects in treating the small-angle scattering. Indeed, the typical space scale for soft fluctuating modes of the electromagnetic field is about the inverse Debye mass $1/m_D \sim 1/e\mu$. This scale is much larger than the typical separation $\sim 1/\mu$ between electrons. From the standpoint of electrons with energy $\sim \mu$, the soft electromagnetic field at the space scale $\sim 1/m_D \gg 1/\mu$ can therefore be viewed as a uniform field at the scale $\sim 1/\mu$. In a uniform field, all electrons in the same spin state scatter the same, and small-angle scattering leads simply to some shift of the distribution function in the momentum space. Any statistics effects are suppressed by some power of the electron charge e. Calculations within the real time thermal field theory performed in [16] corroborate this physical picture of collinear photon emission.

In our approximation of an optically thin medium, the differential radiated energy flux from the electrosphere, $dF/d\omega$, is expressed in terms of the emissitivity as

$$\frac{dF}{d\omega} = \int_0^{h_{max}} dh \frac{dQ(h,\omega)}{d\omega}. \quad (3)$$

For chemical potential (1), the h-integration in (3) can be approximated by the integration over μ as

$$\frac{dF}{d\omega} \approx \sqrt{\frac{3\pi}{2\alpha}} \int_{\mu_{min}}^{\mu(0)} \frac{d\mu}{\mu^2} \frac{dQ(h(\mu),\omega)}{d\omega} \quad (4)$$

with $\mu_{min} = \mu(h_{max})$. In numerical calculations, we take $\mu_{min} = 2m_e$. Of course, the relativistic approximation we made is not good at $\mu \sim m_e$, but the contribution of this region is small, and the corresponding errors are not big.

3. CALCULATION OF $dP/dx\,dL$

The essential ingredient of Eq. (2) is the probability distribution $dP/dx\,dL$ for the photon emission in the electromagnetic field of the electrosphere. Due to the presence of the product $n_F(E)[1-n_F(E')]$ in (2), the

[1)] Physically, the photon formation length (sometimes called the coherence length) is a longitudinal scale at which the photon and electron wave packets become separated. It appears naturally in the LCPI approach [18, 21] formulated in the coordinate space as a dominating scale of the integrals in the longitudinal coordinate.

emissitivity is dominated by the photon emission from electrons near the Fermi surface with $p \sim \mu \gg m_e$. This allows using semiclassical relativistic formulas for the photon spectrum $dP/dx\,dL$. In this paper, we evaluate this spectrum within the LCPI formalism [18, 21]. In this approach, it can be written as

$$\frac{dP}{dx\,dL} = 2\,\mathrm{Re}\int\limits_0^\infty d\xi\,\hat{g}(x)\times$$
$$\times\,[\mathcal{K}(\boldsymbol{\rho}_2,\xi|\boldsymbol{\rho}_1,0) - \mathcal{K}_v(\boldsymbol{\rho}_2,\xi|\boldsymbol{\rho}_1,0)]\Big|_{\boldsymbol{\rho}_1=\boldsymbol{\rho}_2=0}, \quad (5)$$

where

$$\hat{g}(x) = \frac{g_1(x)}{M^2(x)}\,\frac{\partial}{\partial\boldsymbol{\rho}_1}\,\frac{\partial}{\partial\boldsymbol{\rho}_2} + g_2(x) \quad (6)$$

is the spin vertex operator with

$$g_1(x) = \frac{\alpha(1-x+x^2/2)}{x},$$
$$g_2(x) = \frac{\alpha m_e^2 x^3}{2M^2(x)},$$
$$M(x) = px(1-x),$$

$\mathcal{K}$ is the Green's function for a two-dimensional Schrödinger equation with the Hamiltonian

$$\hat{H} = -\frac{1}{2M(x)}\left(\frac{\partial}{\partial\boldsymbol{\rho}}\right)^2 + v(\boldsymbol{\rho}) + \frac{1}{L_0}. \quad (7)$$

Here

$$L_0 = 2M(x)/\epsilon^2, \quad \epsilon^2 = m_e^2x^2 + (1-x)m_\gamma^2,$$

m_γ is the photon quasiparticle mass, and the form of the potential v is given below. In Eqs. (5)–(7), $\boldsymbol{\rho}$ is the coordinate transverse to the electron momentum $\mathbf{p}$, and the longitudinal (along $\mathbf{p}$) coordinate ξ plays the role of time. The function $\mathcal{K}_v$ in (5) is the free Green's function at $v = 0$. We note that at a low density and vanishing mean field, the quantity L_0 coincides with the real photon formation length l_f [18] that characterizes the dominating scale in the ξ-integration in the right-hand side of (5).

The potential in Hamiltonian (7) can be written as

$$v = v_m + v_f.$$

The terms v_m and v_f correspond to the mean and fluctuating components of the vector potential of the electron gas. We note that when l_f is small compared to the scale of variation of μ (along the electron momentum), the ξ-dependence of the potential v can be neglected in evaluating $dP/dx\,dL$. The mean field component is purely real,

$$v_m = -x\mathbf{f}\cdot\boldsymbol{\rho},$$

with

$$\mathbf{f} = e\frac{\partial V}{\partial\boldsymbol{\rho}}$$

(see [21, 27]). It is related to the transverse force from the mean field. Similarly to the classical radiation [28], the effect of the longitudinal force along the electron momentum $\mathbf{p}$ is suppressed by a factor $\sim (m_e/E)^2$, and can be safely neglected. The term v_f can be evaluated similarly to the case of the quark–gluon plasma discussed in [17]. This part is purely imaginary

$$v_f(\boldsymbol{\rho}) = -iP(x\boldsymbol{\rho}),$$

where

$$P(\boldsymbol{\rho}) = e^2\int\limits_{-\infty}^{\infty} d\xi[G(\xi,0_\perp,\xi) - G(\xi,\boldsymbol{\rho},\xi)], \quad (8)$$
$$G(x-y) = u_\mu u_\nu D^{\mu\nu},$$
$$D^{\mu\nu} = \langle A^\mu(x)A^\nu(y)\rangle$$

is the correlation function of the electromagnetic potential (the mean field is assumed to be subtracted) in the electron plasma, and $u_\mu = (1,0,0,-1)$ is the light-cone 4-vector along the electron momentum. We note that the function $P(\boldsymbol{\rho})$ is gauge invariant by construction, and $D^{\mu\nu}$ can be used in any gauge. Formula (8) can be rewritten as (below we replace the argument of $P(\boldsymbol{\rho})$ by $\rho = |\boldsymbol{\rho}|$ since $P(\boldsymbol{\rho})$ does not depend on the direction of the vector $\boldsymbol{\rho}$)

$$P(\rho) = \frac{e^2}{(2\pi)^2}\int d\mathbf{q}_\perp[1-\exp(i\mathbf{q}_\perp\cdot\boldsymbol{\rho})]D(\mathbf{q}_\perp), \quad (9)$$

where the function D is expressed in terms of the correlator G in momentum representation as

$$D(\mathbf{q}_\perp) = \frac{1}{2\pi}\int\limits_{-\infty}^{\infty} dq_0dq_z\delta(q_0-q_z)G(q_0,\mathbf{q}_\perp,q_z). \quad (10)$$

The function $D(\mathbf{q}_\perp)$ can be expressed in terms of the longitudinal and transverse photon self-energies $\Pi_{L,T}$. We use the formulas of the hard dense loop approximation (HDL) for them [30, 31]. The details of the calculations are given in Appendix A.

The function $P(\rho)$ was first introduced in the problem of propagation of relativistic positroniums through amorphous media [29], where the atomic size plays the

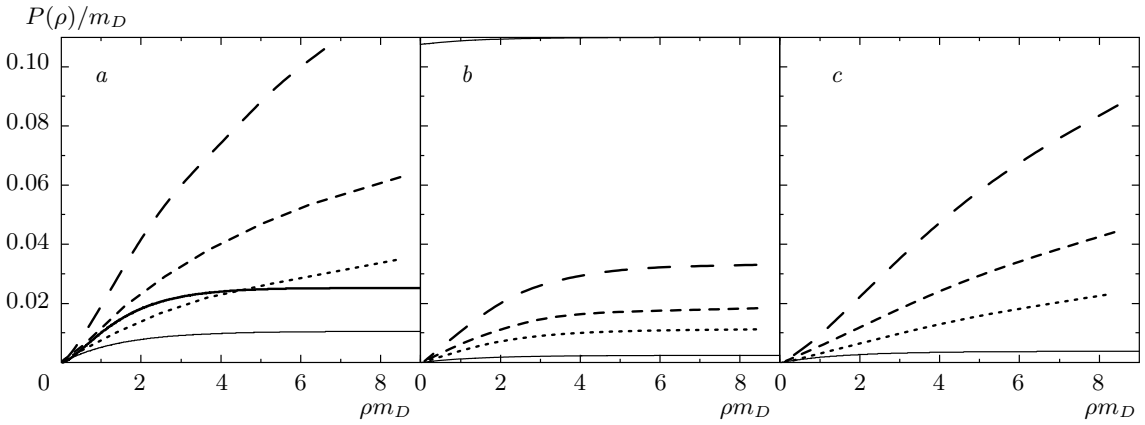

Fig. 1. The function $P(\rho)$ in (9) in units of the Debye mass versus ρm_D for different values of the ratio $\tau = T/m_D$. a — the total $L + T$ contribution, b and c respectively — the longitudinal (L) and transverse (T) contributions. The curves correspond to $\tau = 0$ (solid line), $\tau = 0.5$ (dotted line), $\tau = 1$ (short dashes), and $\tau = 2$ (long dashes). The thick solid line in panel (a) shows the prediction of the static model obtained with dipole cross section (11)

role of the inverse Debye mass. In our approach, the function $P(\rho)$ contains all the information about the electron–electron interaction that is necessary for describing multiple scattering of a given electron in the fluctuating electromagnetic field generated by other electrons. In particular, all the Pauli blocking effects in the process of electron multiple scattering are automatically accumulated in $P(\rho)$. It is worth noting that in the approximation of static Debye-screened scattering centers, the function $P(\rho)$ reduces to $n\sigma(\rho)/2$ [17], where n is the number density of the medium, and

$$\sigma(\rho) = 8\alpha^2 \int d\mathbf{q} \frac{[1 - \exp(i\mathbf{q}\cdot\boldsymbol{\rho})]}{(\mathbf{q}^2 + m_D^2)^2} = \\ = \frac{8\pi\alpha^2}{m_D^2}\,[1 - \rho m_D K_1(\rho m_D)] \quad (11)$$

is the well-known dipole cross section for scattering of an e^+e^- pair of size ρ on the Debye-screened scattering center (and K_1 is the Bessel function). In the static approximation at $\rho \ll 1/m_D$, we can obtain

$$P(\rho) \approx nC\rho^2/2$$

from (11), where

$$C \approx 4\pi\alpha^2 \ln(2/\rho m_D)$$

is a smooth function of ρ. In the limit $\rho \ll 1/m_D$, the function $P(\rho)$ in the HDL approximation also becomes almost quadratic.

The quadratic approximation $P(\rho) \propto \rho^2$ in the LCPI approach is equivalent to the Fokker–Planck approximation in Migdal's approach [21]. It is not very accurate but reasonable for bremsstrahlung in ordinary materials. In this case, the dominating ρ-scale is $\sim 1/m_e x$, and the spectrum is controlled by behavior of $P(\rho)$ at the scale $\sim 1/m_e$, which is much smaller than the screening radius $\sim 1/\alpha m_e Z^{1/3}$ (where Z is the atomic number). For the relativistic electron gas, the situation is quite different. In the dominating ρ-region, the argument of $P(\rho)$ is $\rho \sim (0.1\text{–}2)/m_D$. In this region, $P(\rho)$ is essentially nonquadratic. This is seen well in Fig. 1a, where we plot the results of numerical calculations of $P(\rho)$ for several values of the ratio T/m_D. The results are presented in a dimensionless form. For comparison, we also show the predictions of the static approximation at $T = 0$ (when $m_D = \mu\sqrt{4\alpha/\pi}$) obtained with dipole cross section (11). It can be seen that at $\rho \sim (0.1\text{–}2)/m_D$, the function $P(\rho)$ is almost linear in ρ.

In Figs. 1b,c, to demonstrate the relative effect of the longitudinal and transverse modes, we show the contributions related to Π_L and Π_T separately. We see that at $\rho \lesssim 1/m_D$, the longitudinal and transverse contributions are close to each other. But at $\rho \gtrsim 2/m_D$, the longitudinal part flattens, while the transverse magnetic one continues to increase (for T/m_D not very close to zero). This increase in the transverse part is a consequence of the well-known absence of static magnetic screening in the electron plasma. We note, however, that from the standpoint of the photon emission, the increase in the magnetic contribution with ρ is not important because the photon spectrum is dominated by $\rho \lesssim 1/\epsilon \sim 1/m_D$.

The growth of $P(\rho)$ with temperature is due to the

presence of the Bose–Einstein factor in the function D, Eq. (A.1). It follows from Fig. 1*a* that the prediction of the HDL approximation at $T \ll m_D$, similarly to the static model, flattens at $\rho \gtrsim 2/m_D$. But the static model prediction exceeds the HDL approximately by a factor 2.5. The fact that the static approximation overestimates $P(\rho)$ at $T = 0$ is quite natural, because the Pauli blocking effects reduce the effective number of scatterers. However, it would be incorrect to interpret the increase in $P(\rho)$ with temperature as an artefact associated only with the decrease in the Pauli blocking at high temperatures. The function $P(\rho)$ in the HDL approximation accumulates all the collective effects in soft modes of the electromagnetic field in the electron plasma at the momentum scale $\sim m_D \ll \mu$. In particular, it accounts for the temperature dependence of the density of the plasmon excitations. We note that physically, the appearance of $P(\rho)$ is due to Landau damping of the longitudinal and transverse modes.

It is worth noting that the collective effects cannot be consistently taken into account in the naive modification of the photon propagator in the elastic $e^-e^- \to e^-e^-$ scattering amplitude, as was assumed in [13]. One of the consequence of the inadequacy of this prescription is a strong overestimate of the magnetic contribution in [13]. It is connected with the $1/\theta^4$ (where θ is the scattering angle) behavior of the magnetic contribution to the elastic $e^-e^- \to e^-e^-$ cross section. To perform the θ-integration, the authors of [13] introduced some minimal momentum transfer. In contrast to [13], the magnetic contribution to the function $D(\mathbf{q}_\perp)$ behaves[2)] as $1/\mathbf{q}_\perp^2$ at $\mathbf{q}_\perp \to 0$ and the $\mathbf{q}_\perp$-integration in formula (9) for $P(\rho)$ converges at small $\mathbf{q}_\perp$. This change in the small-angle behavior of the magnetic contribution in our approach compared with the prescription of [13] is connected with the dynamical magnetic screening, which was not consistently accounted for in [13]. In principle, physically, it is evident that the concept of the elastic $e^-e^- \to e^-e^-$ amplitude itself is ill-defined for the momentum transfer $\lesssim m_D$, where the collective effects become significant.

We note that in terms of $P(\boldsymbol{\rho})$, the transverse momentum broadening distribution of an electron propagating over a distance L through the electron gas can be written as [29]

$$I(\mathbf{q}_\perp) = \frac{1}{(2\pi)^2}\int d\boldsymbol{\rho}\exp\left[i\mathbf{q}_\perp\cdot\boldsymbol{\rho} - LP(\rho)\right]. \qquad (12)$$

This formula looks like the prediction of the eikonal approximation, which neglects the variation of the electron tranverse coordinate. But path-integral calculations in [29] show that it is valid beyond the eikonal approximation as well.

We turn to the calculation of the spectrum using (5). Treating v_f as a perturbation, we can write

$$\mathcal{K}(\xi_2,\boldsymbol{\rho}_2|\xi_1,\boldsymbol{\rho}_1) = \mathcal{K}_m(\xi_2,\boldsymbol{\rho}_2|\xi_1,\boldsymbol{\rho}_1) - i\int d\xi\, d\boldsymbol{\rho}\times$$
$$\times\,\mathcal{K}_m(\xi_2,\boldsymbol{\rho}_2|\xi,\boldsymbol{\rho})v_f(\boldsymbol{\rho})\mathcal{K}_m(\xi,\boldsymbol{\rho}|\xi_1,\boldsymbol{\rho}_1) + \ldots, \qquad (13)$$

where $\mathcal{K}_m$ is the Green's function at $v_f = 0$. Then (5) can be written as

$$\frac{dP}{dx\,dL} = \frac{dP_m}{dx\,dL} + \frac{dP_f}{dx\,dL}, \qquad (14)$$

where the first term in the right-hand side comes from $\mathcal{K}_m - \mathcal{K}_v$ in (5) after representing $\mathcal{K}$ in form (13). It corresponds to the photon emission in a smooth mean field. The second term comes from the series in v_f in (13) and can be viewed as the radiation rate due to the electron multiple scattering in the fluctuating field in the presence of a smooth external field.

The analytic expression for the Green's function for the Hamiltonian with a constant force is known (see, e. g., [33]). In our case, $\mathcal{K}_m$ can be written as

$$\mathcal{K}_m(\xi_2,\boldsymbol{\rho}_2|\xi_1,\boldsymbol{\rho}_1) = \frac{M}{2\pi i\xi}\times$$
$$\times\exp\left\{i\left[\frac{M(\boldsymbol{\rho}_2-\boldsymbol{\rho}_1)^2}{2\xi} - \frac{x\xi\mathbf{f}\cdot(\boldsymbol{\rho}_2+\boldsymbol{\rho}_1)}{2} - \right.\right.$$
$$\left.\left. - \frac{x^2\mathbf{f}^2\xi^3}{24M} - \frac{\xi}{L_0}\right]\right\} \qquad (15)$$

with

$$\xi = \xi_2 - \xi_1.$$

With this expression, simple calculations show that Eq. (5) yields a spectrum similar to the well-known semiclassical synchrotron spectrum [34], which can be written in terms of the Airy function

$$\mathrm{Ai}(z) = \frac{1}{\pi}\sqrt{\frac{z}{3}}K_{1/3}(2z^{3/2}/3)$$

(where $K_{1/3}$ is the Bessel function). In the case of interest, for a nonzero photon quasiparticle mass, it is given by [27]

$$\frac{dP_m}{dx\,dL} = \frac{a}{\kappa}\mathrm{Ai}'(\kappa) + b\int\limits_\kappa^\infty dy\mathrm{Ai}(y), \qquad (16)$$

[2)] The same occurs in the hard thermal loop approximation for a hot relativistic plasma with zero chemical potential [32]. We note, however, that a very elegant formula for the analogue of our function $D(\mathbf{q}_\perp)$ obtained in [32] is not valid for a strongly degenerate electron plasma.

where

$$a = -\frac{2\epsilon^2 g_1}{M}, \quad b = M g_2 - \frac{\epsilon^2 g_1}{M}, \quad \kappa = \frac{\epsilon^2}{(M^2 x^2 \mathbf{f}^2)^{1/3}}.$$

Inspecting the longitudinal integrals for the photon radiation in an external field shows that the effective photon formation length for the mean field mechanism is given by

$$\bar{L}_m \approx \min(L_0, L_m),$$

where

$$L_m = (24M/x^2\mathbf{f}^2)^{1/3}$$

(see [27]). A similar estimate can be obtained from the criterion of separation of the photon and electron wave packets. We note that the analytic expression for the Green's function for the oscillator with a constant force is also known (see [33]).

For $P(\rho) \propto \rho^2$, using this Green's function allows obtaining the radiation rate in the form given in [35], where Migdal's approach within the Fokker–Planck approximation was generalized to the case with an external field. The formulas in [35] were used in [15]. However, as was already noted, the approximation $P(\rho) \propto \rho^2$ is clearly not adequate for the electrosphere.

We now discuss the fluctuation component $dP_f/dx\,dL$. We represent it in the form

$$\frac{dP_f}{dx\,dL} = \frac{dP_f^{BH}}{dx} + \frac{dP_f^{LPM}}{dx}, \tag{17}$$

where the first term in the right-hand side corresponds to the leading order in the expansion in v_f in (13), and the second term to the sum of higher-order terms. The expression $dP_f^{BH}/dx\,dL$ is an analogue of the Bethe–Heitler spectrum in ordinary materials, while $dP_f^{LPM}/dx\,dL$ describes the LPM correction. For the Bethe–Heitler term, it follows from (5) and (13) that

$$\frac{dP_f^{BH}}{dx} = 2\int d\boldsymbol{\rho}\, W(x,\boldsymbol{\rho},\mathbf{f}) P(\rho x), \tag{18}$$

$$W(x,\boldsymbol{\rho},\mathbf{f}) = \\ = -\operatorname{Re}\hat{g}(x)\Phi(x,\boldsymbol{\rho},\boldsymbol{\rho}_1,\mathbf{f})\Phi(x,\boldsymbol{\rho},\boldsymbol{\rho}_2,\mathbf{f})\Big|_{\boldsymbol{\rho}_1=\boldsymbol{\rho}_2=0}, \tag{19}$$

$$\Phi(x,\boldsymbol{\rho},\boldsymbol{\rho}',\mathbf{f}) = \int\limits_{-\infty}^{0} d\xi \mathcal{K}_m(\boldsymbol{\rho},0|\boldsymbol{\rho}',\xi). \tag{20}$$

We note that for a nonzero $\mathbf{f}$, the function W cannot be viewed as a probability density for the $|\gamma e\rangle$ Fock component of the physical photon (it is even not positive definite). This is connected with the fact that in an external field, the $|\gamma e\rangle$ Fock component is not stable and decays through the tunnel transition into a free photon and an electron. The analogue of the representation for the LPM correction derived in [19] for a nonzero mean field is given by

$$\frac{dP_f^{LPM}}{dx} = 2\operatorname{Re}\hat{g}(x)\int\limits_0^\infty d\xi \int d\boldsymbol{\rho}\,\Phi(x,\boldsymbol{\rho},\boldsymbol{\rho}_2,\mathbf{f}) \times \\ \times P(\rho x)\tilde{\Phi}(x,\boldsymbol{\rho},\boldsymbol{\rho}_1,\mathbf{f},\xi)\Big|_{\boldsymbol{\rho}_1=\boldsymbol{\rho}_2=0}, \tag{21}$$

where the function $\tilde{\Phi}(x,\boldsymbol{\rho},\boldsymbol{\rho}_1,\mathbf{f},\xi)$ is the solution of the two-dimensional Schrödinger equation with Hamiltonian (7) and with the boundary condition

$$\tilde{\Phi}(x,\boldsymbol{\rho},\boldsymbol{\rho}_1,\mathbf{f},0) = \Phi(x,\boldsymbol{\rho},\boldsymbol{\rho}_1,\mathbf{f})P(\rho x).$$

In the case of zero $\mathbf{f}$, the function W can be written as a density for the $|\gamma e\rangle$ Fock state,

$$W(x,\boldsymbol{\rho}) = \frac{1}{2}\sum_{\{\lambda_i\}} |\Psi(x,\boldsymbol{\rho},\{\lambda_i\})|^2, \tag{22}$$

where $\Psi(x,\boldsymbol{\rho},\{\lambda_i\})$ is the light-cone wave function for the $e \to \gamma e'$ transition and $\{\lambda_i\} = (\lambda_e, \lambda_{e'}, \lambda_\gamma)$ is a set of helicities. We note that contrary to the case $\mathbf{f} \neq 0$, the light-cone wave functions now have definite azimuthal quantum numbers due to the azimuthal symmetry of the Hamiltonian. The LPM correction in this case can also be written in terms of the light-cone wave functions. The results is similar to that for ordinary materials [19, 21]:

$$\frac{dP_f^{LPM}}{dx} = -\operatorname{Re}\sum_{\{\lambda_i\}}\int\limits_0^\infty d\xi \times \\ \times \int d\boldsymbol{\rho}\,\Psi^*(x,\boldsymbol{\rho},\{\lambda_i\})P(\rho x)\tilde{\Phi}(x,\boldsymbol{\rho},\{\lambda_i\},\xi). \tag{23}$$

The boundary condition for $\tilde{\Phi}(x,\boldsymbol{\rho},\{\lambda_i\},\xi)$ is now

$$\tilde{\Phi}(x,\boldsymbol{\rho},\{\lambda_i\},0) = \Psi(x,\boldsymbol{\rho},\{\lambda_i\})P(\rho x).$$

The light-cone wave functions appear in formulas (22) and (23) from the ξ-integrals in (5) and (13) of the Green's function $\mathcal{K}_m$ and from the action of the vertex operator written in terms of the helicity projectors as was done in [17].

The formulas for the light-cone wave functions are given in Appendix B. Using the formulas given there, we can obtain the probability distribution W for the $e \to \gamma e'$ transition at $\mathbf{f} = 0$ as

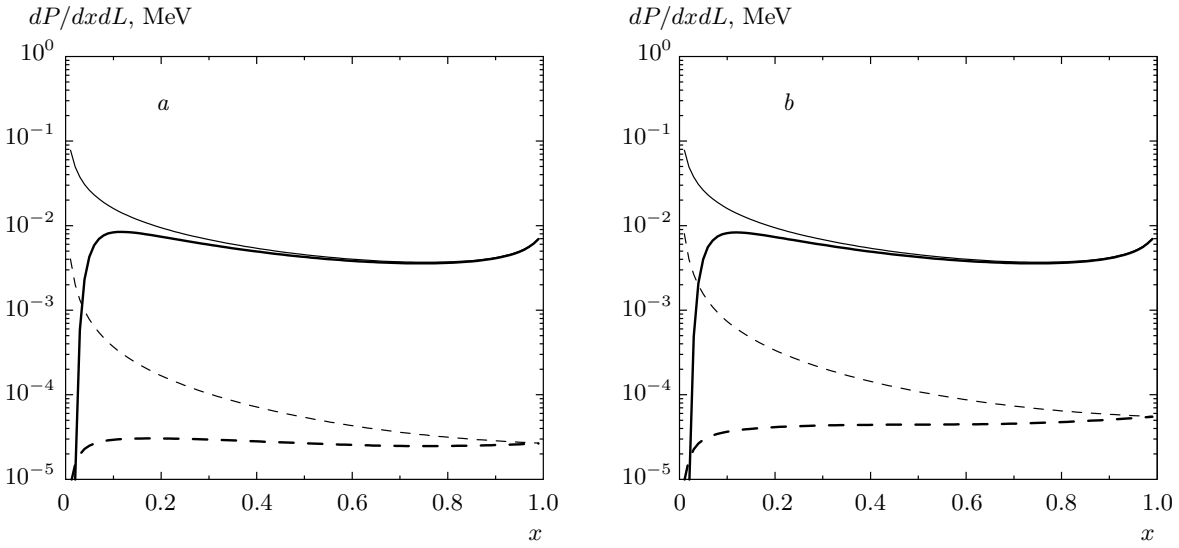

Fig. 2. The contributions to the spectrum $dP/dx\,dL$ from the mean field mechanism (solid line) and the fluctuation mechanism (dashes) for $\mu = 10$ MeV at $T = 0.2$ (a) and 1 (b) MeV. The thick curves are for a nonzero photon mass, and the thin lines are for a massless photon. The contribution of the fluctuation mechanism is calculated using the Bethe–Heitler term with distribution (24)

$$W(x,\boldsymbol{\rho}) = \frac{\alpha}{2\pi^2} \times \\ \times \left\{ \frac{[1+(1-x)^2]}{x}\epsilon^2 K_1^2(\rho\epsilon) + x^3 m_e^2 K_0^2(\rho\epsilon) \right\}, \quad (24)$$

where $K_{0,1}$ are the Bessel functions. Because $K_{0,1}$ decrease exponentially in (24), the dominating ρ scale in formula (18) for the fluctuation term is $\sim 1/\epsilon$.

For a nonzero $\mathbf{f}$, the azimuthal symmetry is absent. This makes the problem considerably more complicated. In this paper, we first calculated the spectrum $dP_f/dx\,dL$ for $\mathbf{f} = 0$. We observed that the LPM correction in (17) is negligible compared to the Bethe–Heitler term. Also, the Bethe–Heitler term itself turns out to be much smaller than the mean field term $dP_m/dx\,dL$. It is clear that a nonzero $\mathbf{f}$ makes $dP_f/dx\,dL$ even smaller. Therefore, an accurate calculation of the fluctuation term for nonzero $\mathbf{f}$ does not make much sense. We have taken the effect of the transverse force into account using qualitative arguments based on the estimates of the coherence lengths with and without a tranverse force. The mean field should suppress the coherence length. The suppression of the radiation rate should be approximately the same [36]. Hence, the mean field suppression factor can be written as the ratio of the formation lengths with and without the mean field. The coherence length in the presence of the mean field is $\sim \bar{L}_m$. Without the mean field in the regime of weak LPM suppression, the coherence length is given by L_0. Therefore, the mean field suppression factor is

$$S_m \approx \bar{L}_m/L_0.$$

We note that due to reduction in the effective formation length, the LPM effect should become even smaller for a nonzero mean field.

To illustrate the relative contributions of the mean field and fluctuation mechanisms to $dP/dx\,dL$, we plot them in Fig. 2 for $\mu = 10$ MeV and $T = 0.2$ and 1 MeV. The mean field part shown in Fig. 2 corresponds to the spectrum averaged over all directions of the electron momentum. The fluctuation contribution was calculated without the mean field suppression factor. The calculations are performed with the k-dependent photon quasiparticle mass extracted from the relation[3)]

$$m_\gamma^2 = \Pi_T(\sqrt{k^2+m_\gamma^2}, k).$$

This gives m_γ increasing from $m_D/\sqrt{3}$ at $k \ll m_D$ to $m_D/\sqrt{2}$ at $k \gg m_D$ with the Debye mass

$$m_D^2 = \frac{4\alpha}{\pi}\left(\mu^2 + \frac{\pi^2}{3}T^2\right).$$

[3)] We ignore the influence of the medium effects on m_e [37] because the photon bremsstrahlung in the region $x \ll 1$, which dominates the emissitivity, is not very sensitive to the electron quasiparticle mass.

It follows from Fig. 2 that the fluctuation contribution is suppressed by a factor $\sim 10^{-2}$. To illustrate the role of a finite photon quasiparticle mass, we also present the results for zero m_γ in Fig. 2 (thin curves). It is seen that the photon mass suppression (usually called the Ter-Mikaelian effect) is very strong at small x. The effect is especially dramatic for the fluctuation part, where the well-known $1/x$ form of the spectrum changes to $\propto x$. This effect was ignored in the analyses in [14, 15], where the massless formulas were used. The results shown in Fig. 2 indicate clearly that the massless approximation is inadequate.

As mentioned previously, our calculations show that for the fluctuation mechanism the LPM suppression is negligible. This contradicts the analysis in [13], where the authors found a very strong LPM suppression (about $\sim 1/300$ at the photon momentum $k = 0.5$ MeV for the electron energy 10 MeV). To calculate the LPM suppression, the authors of [13] used Migdal's formulas with zero photon mass, setting $Z = 1$ there. But it can easily be shown that Migdal's formulas become inapplicable for the electrosphere. We explain this in the language of the LCPI approach. Migdal's approach [24] corresponds in the LCPI formalism to the quadratic parameterization

$$P(\rho) \approx nC\rho^2/2.$$

As described above, this approximation is not accurate for the electrosphere, but is nevertheless suitable for our qualitative analysis. In the quadratic approximation, Hamiltonian (7) takes the oscillator form with

$$\Omega = \sqrt{-inCx^2/M(x)}.$$

The LPM suppression factor S_{LPM} can be written in terms of the dimensionless parameter $\eta = |\Omega|L_0$ [18, 21]. The LPM suppression becomes strong at $\eta \gg 1$. In this limit,

$$S_{LPM} \approx \frac{3}{\eta\sqrt{2}}$$

(see [18]). The LPM effect is negligible for $\eta \ll 1$, when

$$S_{LPM}(\eta) \approx 1 - 16\eta^4/21$$

(see [18]). We note that even at $\eta \sim 1$, the LPM suppression is relatively small because $S_{LPM}(1) \approx 0.86$. A very strong suppression obtained in [13] is mostly due to the neglect of the photon mass. The finite photon mass strongly reduces L_0 and correspondingly the parameter η (by about a factor ~ 400 for $k = 0.5$ and $p \sim 10$ MeV). Also, for the electrosphere, there is no well-known large Coulomb logarithm $\ln(1/\alpha) \sim 5$ (which comes from the logarithm in the dipole cross section [20]) in $|\Omega|$, which is present in Migdal's formulas derived for ordinary materials. Both these effects drastically reduce the value of η for the electrosphere compared to that in Migdal's approach. As a result, the LPM suppression in the electrosphere turns out to be negligible.

4. NUMERICAL RESULTS AND DISCUSSION

In this section, we present numerical results for the emissitivity and radiated energy flux. The results were obtained with some modification of the spectrum $dP/dx\,dL$ in the noncollinear region. As we mentioned above, the collinear approximation we use becomes invalid for very soft photons with $k \lesssim m_\gamma$. In this region, the formalisms [16–18] do not apply. In particular, the LCPI approach [18], which assumes that the transverse momentum integration extends to infinity, should overestimate the photon spectrum at $k \lesssim m_\gamma$. To take this effect into account (at least, qualitatively) in calculating the radiated energy flux, we multiplied $dP/dx\,dL$ by the kinematical suppression factor

$$S_{kin}(k) = 1 - \exp(-k^2/m_\gamma^2).$$

This factor does not give a large effect. It suppresses the radiated energy by ~ 10–$15\,\%$ at $T \approx 0.1$–0.2 MeV and ~ 1–$2\,\%$ at $T \sim 1$ MeV. This shows that the errors from the noncollinear configurations are small.

In Fig. 3, we show the emissitivity for $\mu = 5$ and 10 MeV evaluated at $T = 0.2$ and 1 MeV as a function of ω. We see that the contribution of the mean field emission (the thick solid line) exceeds the fluctuation emission without mean field suppression (dashes) by a factor $\sim 10^2$. The mean field suppression additionally reduces the fluctuation contribution (the thin solid line) by a factor ~ 3–4. We note that there is no photon emission at $\omega < \omega_p^e$ in our semiclasscal approximation at a given μ. For this reason, the differential emissitivity shown in Fig. 3 vanishes abruptly at $\omega = \omega_p^e = m_\gamma$ ($k = 0$). We see from Fig. 3 that despite the Pauli blocking suppression, even at $T = 0.2$ MeV, the contribution of energetic photons with the energy about several units of ω_p^e is important. This demonstrates that the restriction

$$\omega < \sqrt{{\omega_p^e}^2 + m_e^2}$$

for the photon energy imposed by the authors of [13] is clearly inadequate.

In Fig. 4, we plot the differential radiated energy flux $dF/d\omega$ for $\mu(0) = 10$ and 20 MeV obtained at

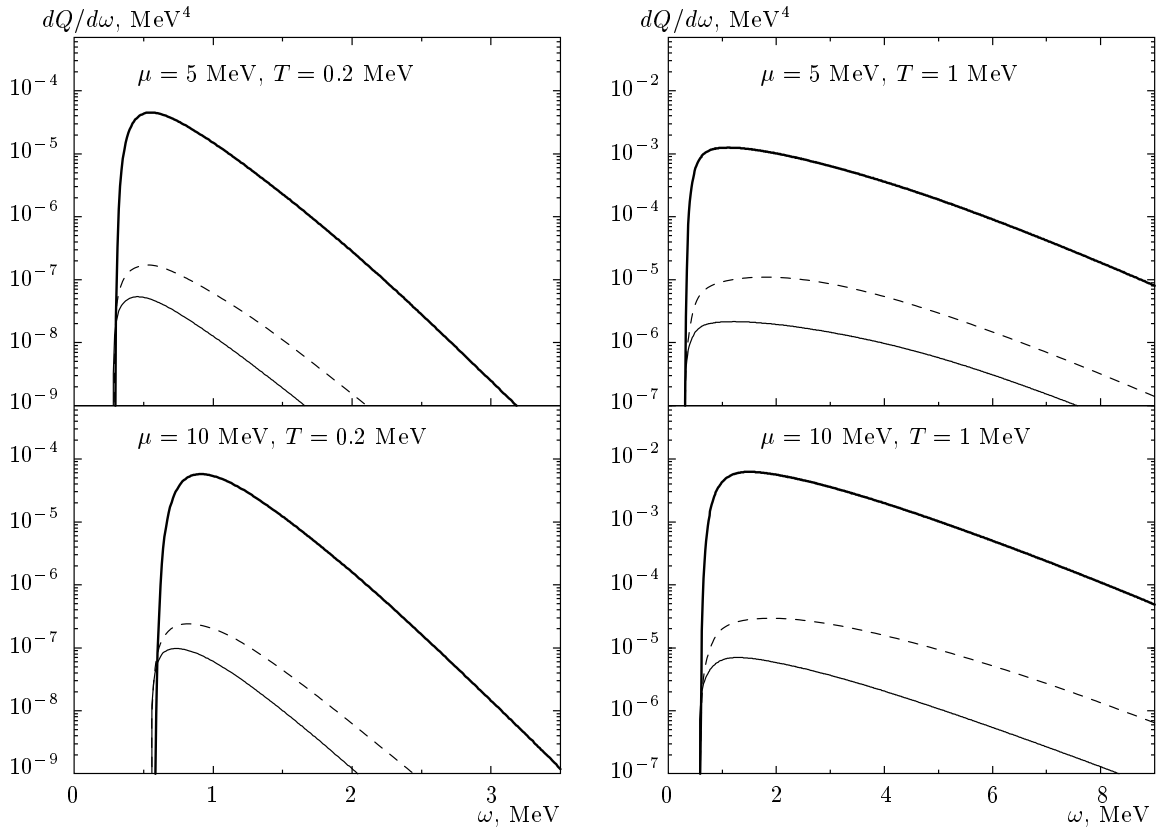

Fig. 3. The emissitivity versus the photon energy ω for $\mu = 5$ and 10 MeV at $T = 0.2$ and 1 MeV. The thick solid line shows the mean field bremsstrahlung. The contribution of the fluctuation mechanism is shown without (dashes) and with (thin solid line) the mean field suppression

$T = 0.2$ and 1 MeV. For the fluctuation contribution, we show the results with and without the mean field suppression factor S_m. For comparison, the black body spectrum is also shown. The mean Coulomb field of the electrosphere reduces the fluctuation term by a factor ~ 3–4. It follows from Figs. 3 and 4 that the relative contribution of the fluctuation mechanism is very small compared to the mean field emission. In some sense, we have a situation similar to that for photon radiation from an atom with a large Z. We note that the form of the spectrum for the mean field mechanism is qualitatively similar to that for the black body radiation.

In Fig. 5, we show the total energy flux

$$F = \int\limits_0^\infty d\omega\, dF/d\omega$$

scaled to the black body radiation as a function of temperature. For comparison, we also plot the predictions for bremsstrahlung obtained in [13–15]. We also show the energy flux from the e^+e^- pair production [4, 10], defined as

$$F_\pm = \int\limits_0^{h_{max}} dh\, Q_\pm(h) \approx \sqrt{\frac{3\pi}{2\alpha}} \int\limits_{\mu_{min}}^{\mu(0)} \frac{d\mu}{\mu^2} Q_\pm(h(\mu))\,. \quad (25)$$

Here, $Q_\pm$ is the energy flux from e^+e^- pairs per unit time and volume. We write it as in [4, 10],

$$Q_\pm = E_{e^+e^-}\, dN_{e^+e^-}/dt\, dV,$$

where

$$E_{e^+e^-} \approx 2(m_e + T)$$

is the typical energy of e^+e^- pairs and $dN_{e^+e^-}/dt\, dV$ the rate of e^+e^- pair production per unit time and volume given by

$$\frac{dN_{e^+e^-}}{dt\, dV} \approx \frac{3T^3\mu}{2\pi^3}\sqrt{\frac{\alpha}{\pi}} \exp\left(-\frac{2m_e}{T}\right) J(\xi) \quad (26)$$

with

$$\xi = \frac{2\mu}{T}\sqrt{\frac{\alpha}{\pi}},$$

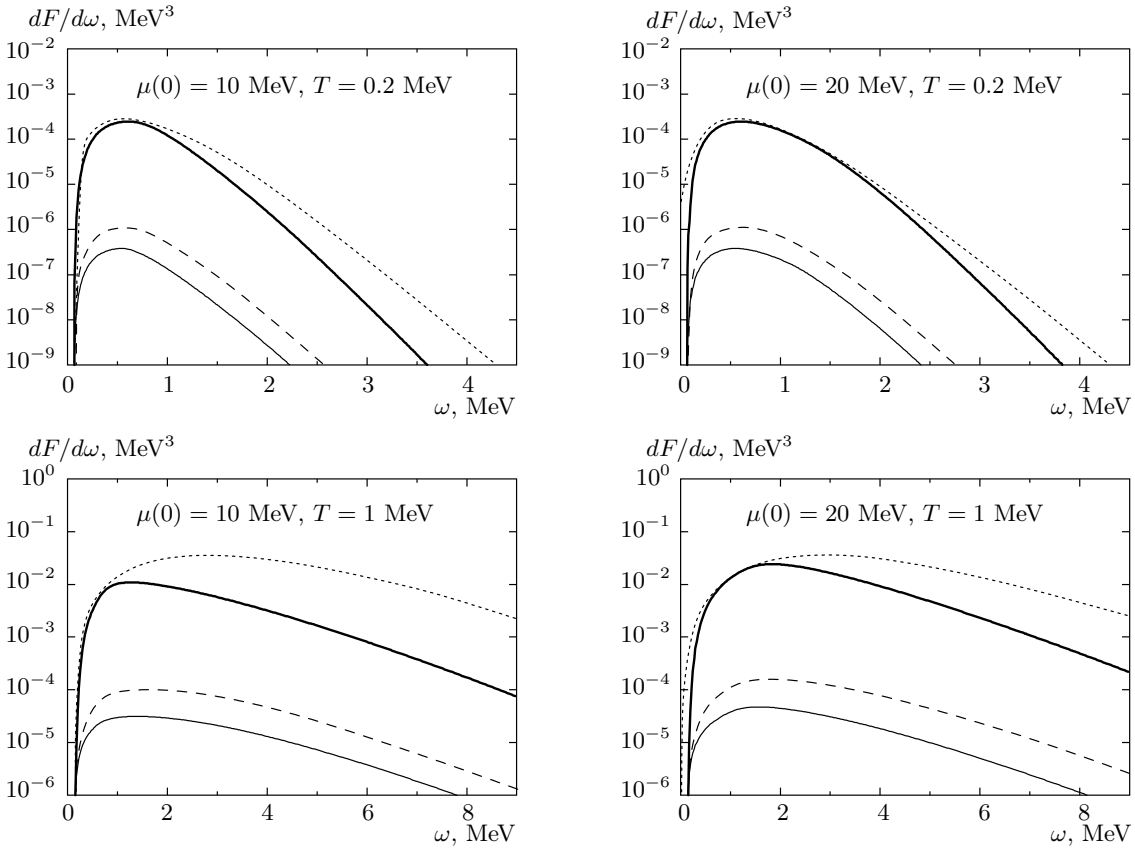

Fig. 4. The differential radiated energy flux from the electrosphere for the mean field bremsstrahlung (thick solid line) and for the Bethe–Heitler bremsstrahlung with (thin solid line) and without (dashes) the mean field suppression. The dotted lines show the black body spectrum

and the function J is defined as in [10]:

$$J(x) = \frac{x^3 \ln(1+2/x)}{3(1+0.074x)^3} + \frac{\pi^5 x^4}{6(13.9+x)^4}\,.$$

We see from Fig. 5 that in the region $T \sim 0.1$–1 MeV, the mean field photon emission considerably exceeds both the fluctuation bremsstrahlung and the energy flux from e^+e^- pair production.

Figures 4 and 5 demonstrate that the energy flux from the mean field photon emission may be of the same order of magnitude as the black body radiation. In other words, the approximation of an optically thin electrosphere is not very good, and the photon absorption and stimulated emission may be important. But because the radiation rate we obtained does not exceed the black body limit, they cannot modify our results strongly. We note that the authors of [15] obtained the energy flux for $T \lesssim 1$ MeV considerably exceeding the black body limit. This can be seen from Fig. 5, where the results in [15] at $\mu(0) = 20$ MeV are shown. The authors of [15] claim that the electrosphere may radiate stronger than a black body. This statement is obviously incorrect. The violation of the black body limit in [15] is just a signal that the thin-medium approximation becomes inapplicable at high emissitivity. As regards the very large emissitivity obtained in [15], we have already mentioned that it may be due to an incorrect description of the Pauli blocking and neglect of the photon mass.

As mentioned above, our assumption that the photon emission is a local process is valid if $l_f \sim \bar{L}_m \ll L_{el}$, where L_{el} is the typical scale of variation of the potential v_m along the electron trajectory. For chemical potential (1), it can be defined as

$$L_{el} \approx H\mu(0)/\mu(h)\cos\theta,$$

where θ is the angle between the electron momentum and the star surface normal. Evidently, the contribution of the configurations with $\bar{L}_m \gtrsim L_{el}$ to the photon

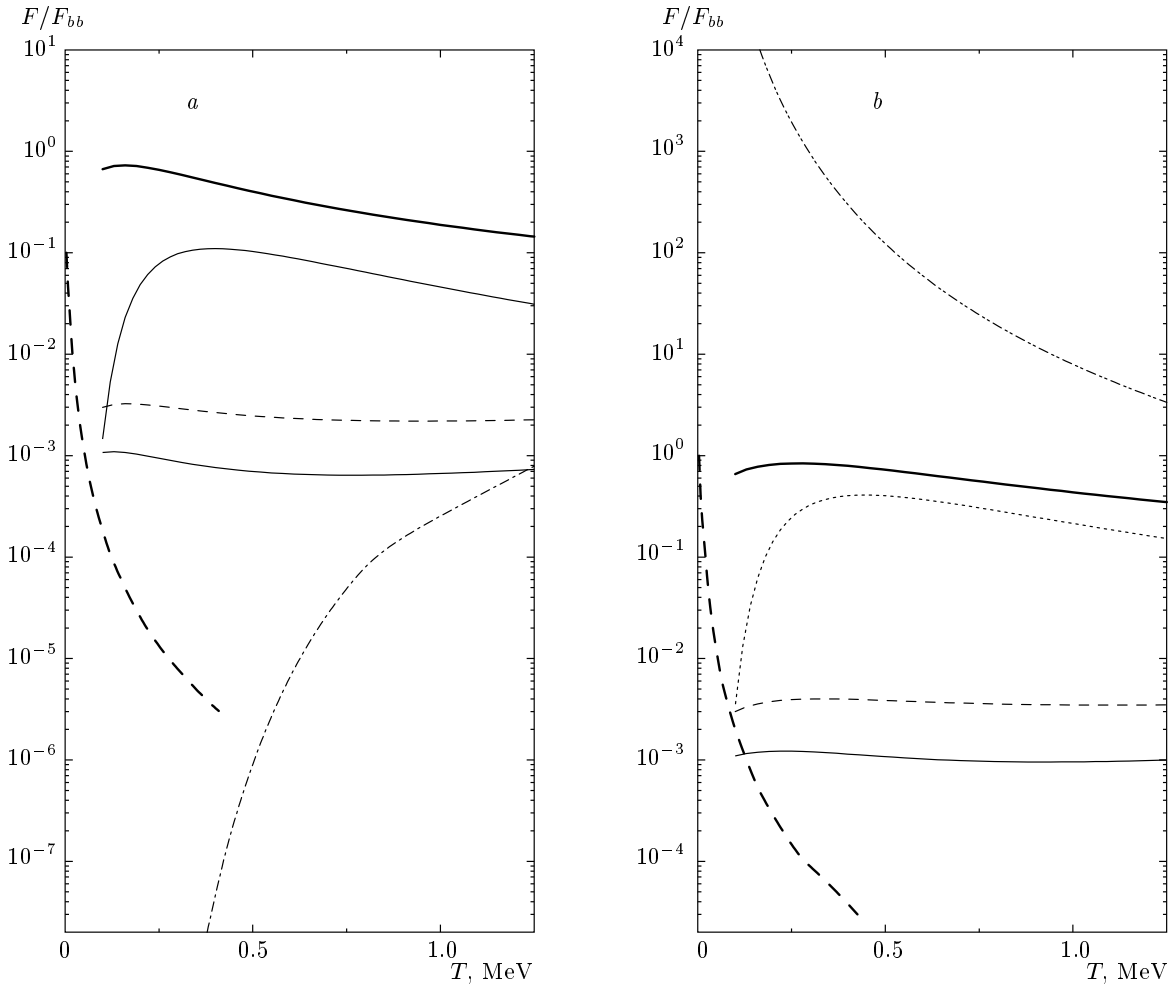

Fig. 5. The total radiated energy flux (scaled to the black body radiation) from the electrosphere for the mean field bremsstrahlung (thick solid line) and for the Bethe–Heitler bremsstrahlung with (thin solid line) and without (short dashes) the mean field suppression. The contribution from the tunnel e^+e^- creation [4, 10] evaluated using (25) is also shown (dotted line). The long dashes show the results for the $e^- + e^- \to e^- + e^- + \gamma$ process obtained in [13]. The dot-dashed lines show the results for the same process in [14]. The dot-dot-dashed line shows the bremsstrahlung contribution with inclusion of the mean Coulomb field in [15]. $\mu(0) = 10$ (a), 20 (b) MeV

spectrum are to be suppressed by the finite-size suppression factor

$$S_{fs} \approx \min(L_{el}, \bar{L}_m)/\bar{L}_m.$$

We verified numerically that this suppression factor gives a negligible effect. This justifies the local approximation.

According to the simulation of the thermal evolution of young quark stars performed in [25], the temperature at the star surface becomes ~ 0.2 MeV at $t \sim 1$ s. But the mean field bremsstrahlung was not taken into account in the analysis in [25]. In the light of our results, we can expect that the cooling of the bare quark star surface should proceed somewhat faster than predicted in [25]. It is worth noting that in the initial stage of the quark star evolution, the mean field photon emission can only modify the temperature near the star surface. The evolution of the star core temperature is driven by neutrino emission [25] because the neutrino luminosity is much larger than the photon (and e^+e^-) luminosity for an extended period of time [25]. The higher luminosity due to the mean field bremsstrahlung increases the possibility for detecting bare quark stars. From the standpoint of light curves at $t \gtrsim 1$ s, it would also be interesting to investigate the mean field bremsstrahlung for $T \lesssim 0.1$ MeV. Ho-

wever, the photon emission from the nonrelativistic region of the electrosphere may be important at such temperatures, where our formulas become inapplicable. As regards the contribution of the relativistic region $\mu \gg m_e$, extrapolation of the curves shown in Fig. 5 to $T \lesssim 0.1$ MeV allows expecting that the mean field emission will dominate the energy flux at lower temperatures as well.

A remark is in order on the photon distribution seen by a distant observer. For the obtained values of the energy flux, the radiation cannot stream outward freely. The point is that near the star surface, the thermalization time in the comoving frame for the $e^+e^-\gamma$ wind is negligibly small compared to the star radius. This follows from estimates of the mean free path λ related to the $\gamma + e^\pm \to \gamma + e^\pm$ and $\gamma + \gamma \leftrightarrow e^+ + e^-$ processes. Qualitative calculations give $\lambda \sim 10^{-3}$cm at $T \sim 0.1$ MeV and $\lambda \sim 10^{-6}$cm at $T \sim 1$ MeV. Therefore, the $e^+e^-\gamma$ wind can be described as a hydrodynamical flow. The hydrodynamical description is valid up to the freeze-out surface, beyond which the radiation streams outward almost freely. For an observer at a large distance from the star, the photon spectrum is close to the black body one with the temperature $T_{ext} = T_{fr}\Gamma_{fr}$, where T_{fr} is the wind temperature and Γ_{fr} is the bulk Lorentz factor of the wind at the freeze-out level [38, 39]. It can be shown that for a relativistic wind [38, 39]

$$T_{fr}\Gamma_{fr} \approx T_i\Gamma_i,$$

where T_i is the wind temperature after its thermalization and Γ_i is the bulk Lorentz factor of the wind near the star surface. For $T \sim 0.1$ MeV, the electron fraction in the $e^+e^-\gamma$ wind is small after thermalization. Simple qualitative calculations then give

$$T_i\Gamma_i \approx T(3\kappa\Gamma_i^2/16)^{1/4},$$

where

$$\kappa = (F + F_\pm)/F_{bb}.$$

As a plausible estimate, we can take $\Gamma_i^2 \approx 3$ and $\kappa \approx 1$. Then $T_{ext} \approx 0.85T$. For $T \sim 1$ MeV, the electron fraction in the wind after thermalization becomes close to that for a relativistic plasma. In this case,

$$T_i\Gamma_i \approx T(3\kappa\Gamma_i^2/44)^{1/4}.$$

Taking $\kappa \approx 0.4$, we obtain $T_{ext} \approx 0.5T$. We note that in both cases, the fraction of $e^\pm$ pairs in the wind is negligibly small beyond the freeze-out surface [39].

We note that our calculations probably do not apply to quark stars in the color flavor-locked (CFL) superconducting phase. It was suggested previously [40] that despite the absence of electrons in the bulk SQM in the CFL phase, the electrosphere may exist due to the surface quark charge [41]. However, the recent analysis in [42] gives evidence in favor of the absence of such a surface charge. But for the CFL phase, a significant photon emission from the SQM itself may exist due to the photon–gluon mixing [43]. The results in [43] show that this radiation is comparable to the black body limit. Because we also obtain the radiation rate comparable to the black body radiation, it may be difficult to distinguish a bare quark star in the CFL phase from that in the normal (or 2SC) phase.

5. CONCLUSION

We have evaluated the photon emission from the electrosphere of a bare quark star (in the normal or 2SC phase). The analysis is based on the LCPI reformulation [17] of the AMY approach [16] to the photon emission from relativistic plasmas. The developed approach, in contrast to the previous qualitative studies [13–15], for the first time allows giving a robust treatment of the Pauli blocking effects in photon bremsstrahlung. We demonstrate that for the temperatures $T \sim$ 0.1–1 MeV, the dominating contribution to the photon emission is due to bending of electron trajectories in the mean electric field of the electrosphere. The energy flux from the mean field photon emission is of the order of the black body limit. Our results show that the contribution of the Bethe–Heitler bremsstrahlung due to the electron–electron interaction is negligible compared to the mean field photon emission. Contrarily to [13], we demonstrate that the LPM suppression is negligible.

The energy flux related to the mean field bremsstrahlung also turns out to be larger than that from the tunnel e^+e^- pair creation [4, 10]. In the light of these results, the situation with distinguishing bare quark stars made of SQM in the normal (or 2SC) phase from neutron stars may be more optimistic than in the scenario with the tunnel e^+e^- creation discussed in [25].

I thank J. F. Caron for providing the file for the radiated energy flux obtained in [14]. I am also grateful to T. Harko and D. Page for communication. This work was supported in part by the grant № SS-6501.2010.2.

APPENDIX A

Calculation of the function $D(\mathbf{q}_\perp)$

In this appendix, we discuss the calculation of the function $D(\mathbf{q}_\perp)$. To evaluate this function, we need to know the correlator $D^{\mu\nu}$. In momentum representation, we can obtain

$$D^{\mu\nu}(q) = -2[1 + n_B(q_0)]\,\mathrm{Im}\,D_r^{\mu\nu}(q)\,,$$

where

$$n_B = [\exp(q_0/T) - 1]^{-1}$$

is the Bose–Einstein factor and $D_r^{\mu\nu}(q)$ is the retarded Green's function. As was already noted, the function $P(\rho)$ is gauge invariant, and we can use $D_r^{\mu\nu}$ in any gauge. Expressing the retarded propagator in the Coulomb gauge in terms of longitudinal and transverse photon self-energies, we obtain

$$D(\mathbf{q}_\perp) = -\frac{1}{\pi}\int\limits_{-\infty}^{\infty} dq_0 \frac{\exp(q_0/T)}{\exp(q_0/T)-1} \times$$
$$\times \left\{ \frac{\mathrm{Im}\,\Pi_L(q_0,\mathbf{q})}{[\mathbf{q}^2 - \mathrm{Re}\,\Pi_L(q_0,\mathbf{q})]^2 + (\mathrm{Im}\,\Pi_L(q_0,\mathbf{q}))^2} + \frac{\mathbf{q}_\perp^2}{\mathbf{q}^2} \times \right.$$
$$\left. \times \frac{\mathrm{Im}\,\Pi_T(q_0,\mathbf{q})}{[\mathbf{q}_\perp^2 + \mathrm{Re}\,\Pi_T(q_0,\mathbf{q})]^2 + (\mathrm{Im}\,\Pi_T(q_0,\mathbf{q}))^2} \right\}\Bigg|_{q_z=q_0}. \quad (A.1)$$

In numerical calculations, we use the HDL expressions [30, 31] for $\Pi_{L,T}$:

$$\Pi_L(q_0,\mathbf{q}) = m_D^2\left[\frac{q_0}{2q}\ln\left(\frac{q_0+q}{q_0-q}\right) - 1\right], \quad (A.2)$$

$$\Pi_T(q_0,\mathbf{q}) = \frac{m_D^2}{2}\left[\frac{q_0^2}{q^2} + \frac{(q^2-q_0^2)q_0}{2q^3}\ln\left(\frac{q_0+q}{q_0-q}\right) - 1\right] \quad (A.3)$$

with the Debye mass

$$m_D^2 = \frac{4\alpha}{\pi}\left(\mu^2 + \frac{\pi^2 T^2}{3}\right).$$

APPENDIX B

Formulas for the light-cone wave functions

For zero $\mathbf{f}$, the light-cone wave functions have a definite orbital quantum number m. As was mentioned, the light-cone wave functions appear from the longitudinal integrals of the Green's function. For $\mathbf{f} = 0$, it is the free Green's function given by

$$\mathcal{K}_v(\xi_2,\boldsymbol{\rho}_2|\xi_1,\boldsymbol{\rho}_1) = \frac{M}{2\pi i\xi}\exp\left\{i\left[\frac{M(\boldsymbol{\rho}_2-\boldsymbol{\rho}_1)^2}{2\xi} - \frac{\xi\epsilon^2}{2M}\right]\right\} \quad (B.1)$$

with $\xi = \xi_2 - \xi_1$. The ξ-integration can be performed using the relation

$$\int\limits_{-\infty}^{0} d\xi\,\mathcal{K}_v(\boldsymbol{\rho}_2,0|\boldsymbol{\rho}_1,\xi) = -\frac{iM}{\pi}K_0(|\boldsymbol{\rho}_2-\boldsymbol{\rho}_1|\epsilon)\,, \quad (B.2)$$

where K_0 is the Bessel function. Then the light-cone wave functions can be written in terms of the Bessel functions K_0 and K_1. After representing vertex operator (6) in terms of the helicity state projectors as in [17], we obtain

$$\Psi(x,\boldsymbol{\rho},\lambda_e,\lambda_{e'},\lambda_\gamma) = \frac{1}{2\pi}\times$$
$$\times\sqrt{\frac{\alpha}{2x}}\,[\lambda_\gamma(2-x) + 2\lambda_e x]\exp(-i\lambda_\gamma\varphi)\epsilon K_1(\rho\epsilon) \quad (B.3)$$

for $\lambda_{e'} = \lambda_e$, where φ is the azimuthal angle. For $\lambda_{e'} = -\lambda_e$, we obtain

$$\Psi(x,\boldsymbol{\rho},\lambda_e,-\lambda_e,2\lambda_e) = \frac{-i}{2\pi}\sqrt{2\alpha x^3}\,m_e K_0(\rho\epsilon)\,. \quad (B.4)$$

REFERENCES

1. E. Witten, Phys. Rev. D **30**, 272 (1984).
2. C. Alcock, E. Farhi, and A. Olinto, Astrophys. J. **310**, 261 (1986).
3. P. Haensel, J. L. Zdunik, and R. Schaeffer, Astron. Astrophys. **160**, 121 (1986).
4. V. V. Usov, Phys. Rev. Lett. **80**, 230 (1998) [arXiv: astro-ph/9712304].
5. C. Kettner, F. Weber, and M. K. Weigel, Phys. Rev. D **51**, 1440 (1995).
6. T. Chmaj, P. Haensel, and W. Slominski, Nucl. Phys. B **24**, 40 (1991).
7. K. S. Cheng and T. Harko, Astrophys. J. **596**, 451 (2003) [arXiv:astro-ph/0306482].
8. V. V. Usov, Phys. Rev. Lett. **87**, 021101 (2001).
9. A. R. Zhitnitsky, JCAP **0310**, 010 (2003) [arXiv:hep-ph/0202161]; M. M. Forbes and A. R. Zhitnitsky, JCAP **0801**, 023 (2008) [arXiv:astro-ph/0611506]; M. M. Forbes and A. R. Zhitnitsky, Phys. Rev. D **78**, 083505 (2008).

10. V. V. Usov, Astrophys. J. **550**, L179 (2001) [arXiv: astro-ph/0103361].

11. J. Schwinger, Phys. Rev. **82**, 664 (1951).

12. A. G. Aksenov, M. Milgrom, and V. V. Usov, Astrophys. Space Sci. **308**, 613 (2007) [arXiv:astro-ph/0606613].

13. P. Jaikumar, C. Gale, D. Page, and M. Prakash, Phys. Rev. D **70**, 023004 (2004).

14. J. F. Caron and A. R. Zhitnitsky, Phys. Rev. D **80**, 123006 (2009).

15. T. Harko and K. S. Cheng, Astrophys. J. **622**, 1033 (2005) [arXiv:astro-ph/0412280].

16. P. Arnold, G. D. Moore, and L. G. Yaffe, JHEP **0111**, 057 (2001); JHEP **0112**, 009 (2001); JHEP **0206**, 030 (2002).

17. P. Aurenche and B. G. Zakharov, JETP Lett. **85**, 149 (2007) [arXiv:hep-ph/0612343].

18. B. G. Zakharov, JETP Lett. **63**, 952 (1996).

19. B. G. Zakharov, JETP Lett. **64**, 781 (1996).

20. B. G. Zakharov, Phys. Atom. Nucl. **62**, 1008 (1999) [arXiv:hep-ph/9805271].

21. B. G. Zakharov, Phys. Atom. Nucl. **61**, 838 (1998) [arXiv:hep-ph/9807540].

22. B. G. Zakharov, Nucl. Phys. Proc. Suppl. **146**, 151 (2005) [arXiv:hep-ph/0412177].

23. L. D. Landau and I. Ya. Pomeranchuk, Dokl. Akad. Nauk SSSR **92**, 535, 735 (1953).

24. A. B. Migdal, Phys. Rev. **103**, 1811 (1956).

25. D. Page and V. V. Usov, Phys. Rev. Lett. **89**, 131101 (2002) [arXiv:astro-ph/0204275].

26. B. G. Zakharov, Phys. Lett. B **690**, 250 (2010) [arXiv:hep-ph/1003.5770].

27. B. G. Zakharov, JETP Lett. **88**, 475 (2008) [arXiv: hep-ph/0809.0599].

28. L. D. Landau and E. M. Lifshitz, *The Classical Theory of Fields*, Pergamon Press (1975).

29. B. G. Zakharov, Sov. J. Nucl. Phys. **46**, 92 (1987).

30. E. Braaten, Can. J. Phys. **71**, 215 (1993) [arXiv: hep-ph/9303261].

31. E. Braaten and D. Segel, Phys. Rev. D **48**, 1478 (1993) [arXiv:hep-ph/9302213].

32. P. Aurenche, F. Gelis, and H. Zaraket, JHEP **0205**, 043 (2002) [arXiv:hep-ph/0204146].

33. R. P. Feynman and A. Hibbs, *Quantum Mechanics and Path Integrals*, McGraw Hill, New York (1965).

34. V. N. Baier and V. M. Katkov, JETP **26**, 854 (1968).

35. V. G. Baryshevskii and V. V. Tikhomirov, JETP **63**, 116 (1986).

36. V. M. Galitsky and I. I. Gurevich, Il Nuovo Cim. **32**, 396 (1964).

37. J. P. Blaizot and J. Y. Ollitrault, Phys. Rev. D **48**, 1390 (1993).

38. B. Paczynski, Astrophys. J. **308**, L43 (1986).

39. O. M. Grimsrud and I. Wasserman, arXiv:astro-ph/9805138.

40. V. V. Usov, Phys. Rev. D **70** 067301 (2004).

41. J. Madsen, Phys. Rev. Lett. **87**, 172003 (2001).

42. M. Oertel and M. Urban, Phys. Rev. D **77**, 074015 (2008).

43. C. Vogt, R. Rapp, and R. Ouyed, Nucl. Phys. A **735**, 543 (2004).